HAL open science

Physical, Thermal, and Spectroscopic Characterization of Biofield Energy Treated Potato Micropropagation Medium

Mahendra Kumar Trivedi, Alice Branton, Dahryn Trivedi, Gopal Nayak, Khemraj Bairwa, Snehasis Jana

To cite this version:

Mahendra Kumar Trivedi, Alice Branton, Dahryn Trivedi, Gopal Nayak, Khemraj Bairwa, et al.. Physical, Thermal, and Spectroscopic Characterization of Biofield Energy Treated Potato Micropropagation Medium. American Journal of Bioscience and Bioengineering, 2015, 3 (5), pp.106-113. hal-01465824

HAL Id: hal-01465824

https://hal.science/hal-01465824v1

Submitted on 13 Feb 2017

HAL is a multi-disciplinary open access archive for the deposit and dissemination of scientific research documents, whether they are published or not. The documents may come from teaching and research institutions in France or abroad, or from public or private research centers.

L'archive ouverte pluridisciplinaire **HAL**, est destinée au dépôt et à la diffusion de documents scientifiques de niveau recherche, publiés ou non, émanant des établissements d'enseignement et de recherche français ou étrangers, des laboratoires publics ou privés.

Distributed under a Creative Commons Attribution 4.0 International License

American Journal of Bioscience and Bioengineering
2015; 3(5): 106-113
Published online November 9, 2015 (http://www.sciencepublishinggroup.com/j/bio)
doi: 10.11648/j.bio.20150305.24
ISSN: 2328-5885 (Print); ISSN: 2328-5893 (Online)

Physical, Thermal, and Spectroscopic Characterization of Biofield Energy Treated Potato Micropropagation Medium

Mahendra Kumar Trivedi[1], Alice Branton[1], Dahryn Trivedi[1], Gopal Nayak[1], Khemraj Bairwa[2], Snehasis Jana[2, *]

[1]Trivedi Global Inc., Henderson, NV, USA
[2]Trivedi Science Research Laboratory Pvt. Ltd., Bhopal, Madhya Pradesh, India

Email address:
publication@trivedisrl.com (S. Jana)

To cite this article:
Mahendra Kumar Trivedi, Alice Branton, Dahryn Trivedi, Gopal Nayak, Khemraj Bairwa, Snehasis Jana. Physical, Thermal, and Spectroscopic Characterization of Biofield Energy Treated Potato Micropropagation Medium. *American Journal of Bioscience and Bioengineering*. Vol. 3, No. 5, 2015, pp. 106-113. doi: 10.11648/j.bio.20150305.24

Abstract: Potato Micropropagation Medium (PMM) is the growth medium used for *in vitro* micropropagation of potato tubers. The present study was intended to assess the effect of biofield energy treatment on the physical, thermal and spectroscopic properties of PMM. The study was attained in two groups *i.e.* control and treated. The control group was remained as untreated, while the treated group was received Mr. Trivedi's biofield energy treatment. Finally, both the samples (control and treated) were evaluated using various analytical techniques such as X-ray diffractometry (XRD), differential scanning calorimetry (DSC), thermogravimetric analysis- differential thermal analysis (TGA-DTA), UV-Vis spectrometry, and Fourier transform infrared (FT-IR) spectroscopy. The XRD analysis showed the crystalline nature of both control and treated samples of PMM. The X-ray diffractogram showed the significant increase in the intensity of XRD peaks in treated sample as compared to the control. The XRD analysis revealed 6.64% increase in the average crystallite size of treated PMM with respect to the control. The DSC analysis showed about 8.66% decrease in the latent heat of fusion in treated sample with respect to the control. The TGA-DTA analysis exhibited about 4.71% increase in onset temperature of thermal degradation after biofield treatment with respect to the control, while the maximum thermal degradation temperature (T_{max}) was also increased (5.06%) in treated sample with respect to the control. This increase in T_{max} might be correlated with increased thermal stability of treated sample as compared to the control. The UV spectroscopic study showed the slight blue shift in λ_{max} of treated sample with respect to the control. FT-IR spectrum of control PMM showed the peak at 3132 cm^{-1} (C-H stretching) that was observed at higher wavenumber *i.e.* at 3161 cm^{-1} in the treated sample. Other vibrational peaks in the treated sample were observed in the similar region as that of the control. Altogether, the XRD, DSC, TGA-DTA, UV-Vis, and FT-IR analysis suggest that Mr. Trivedi's biofield energy treatment has the impact on physicochemical properties of PMM. This treated PMM might be more effective as a micropropagation medium as compared to the control.

Keywords: Biofield Energy Treatment, Potato Micropropagation Medium, X-ray Diffraction, Differential Scanning Calorimetry (DSC), UV-vis Spectroscopy, Fourier Transform Infrared Spectroscopy

1. Introduction

Micropropagation is the technique of rapidly multiplying the stock plant material to generate a number of progeny plants, using advanced plant tissue culture methods [1, 2]. This method is used to multiply novel plants, such as genetically modified, bred of conventional plant, plants that do not produce seeds *etc.* [3, 4]. The potato (*Solanum tuberosum* L.) is one of the vegetable plant belongs to *Solanaceae* family. Conventionally, potato is propagated using tubers that have low multiplication ratio of about 1:4 [5, 6]. The current progression in tissue culture techniques, specifically micropropagation led to a new method of propagation through *in vitro* techniques [7]. The micropropagation medium used for propagation of potato is termed as potato micropropagation medium (PMM). It contains ammonium nitrate and potassium nitrate as the source of nitrate; kinetin and indole acetic acid as the plant growth regulators. Apart from this, it also consists with mineral salts, vitamins, and amino acids, which are required

for the proper growth and development of propagated potato tuber [6, 8]. Despite lots of advantages of micropropagation technique, it is a costly approach and required extensive care at every step. Therefore, an alternate approach is required, which can enhance the nutrient value and propagation capacity of PMM used for potato micropropagation. Recently, biofield energy treatment has been studied in the several fields and reported as an alternate method for alteration of numerous properties of living organisms and non-living things [9, 10].

Biofield energy treatment is the part of energy therapy. The National Institute of Health/National Center for Complementary and Alternative Medicine (NIH/NCCAM) considered the healing energy (putative energy fields) treatment under the subcategory of energy therapies [11]. These energy therapies (healing touch, magnet therapy, bio-electromagnetic therapy *etc*. involve low-level of energy field interactions [12]. The human body is an incredible biological quantum "machine" possessing the bioenergetics field that has incredible potential. The human bioenergetic field consisted with energy structures like bio-photon [13]. These energy structures contain information, which regulate and help all the system of human body to communicate and work coherently [14]. In the healthy condition, these biophotons are coherent and work with the natural frequencies of our body and the Earth. In diseased condition, these biophotons aren't ordered, resulting in communication problems among our cells, organs, and energy systems [15]. It is evidently seen in the cancer cells that are so discordant with rest of the cells of the body, resulting in uncontrolled growth and endangering the survival of the body [16]. The practitioners of energy medicine manipulate and balance this bioenergetic field *via* harnessing the energy from the Universe [17]. Thus, the biofield energy treatment is the process in which, the human harness the energy from environment or universe and transmit to any living or nonliving object on the Globe. Mr. Trivedi is known to possess a unique biofield energy treatment, known as The Trivedi Effect®. Recently, Mr. Trivedi's biofield energy treatment is reported to increase the overall growth of plants and quality and quantity of plant products like ginseng, blueberry, tomato, *etc.* even in the absence of pesticides and fertilizers [18, 19]. The biofield treated plants exhibited an early tendency of germination, rooting, and rapid maturation. The contents of chlorophyll (a and b), and total chlorophyll were also found increased in the treated plants as compared to the control [20]. Moreover, the biofield treatment has also reported to alter the physicochemical and spectral properties of organic products such as beef extract and meat infusion powder [21].

Hence, after considering the impact of biofield treatment, the present study was aimed to evaluate the impact of biofield treatment on the PMM. The analysis was done using various analytical techniques such as X-ray diffractometry (XRD), differential scanning calorimetry (DSC), thermogravimetric analysis-differential thermal analysis (TGA-DTA), UV-Vis spectrometry, and Fourier transform infrared (FT-IR) spectroscopy.

2. Materials and Methods

2.1. Study Design

Potato micropropagation medium (PMM, Table 1) was obtained from HiMedia Laboratories, India. The PMM sample was divided into two groups *i.e.* control and treated.

Table 1. *Chemical composition of potato micropropagation medium.*

S. No.	Ingredients	Mg/Liter
1	Potassium nitrate	1900
2	Ammonium nitrate	1650
3	Calcium chloride. $2H_2O$	440
4	Magnesium sulphate	180.68
5	Potassium phosphate monobasic	170
6	Myo-Inositol	100
7	EDTA disodium salt. $2H_2O$	37.3
8	Ferrous sulphate. $7H_2O$	27.8
9	Manganese sulphate. H_2O	16.89
10	Zinc sulphate. $7H_2O$	8.6
11	Boric acid	6.2
12	Glycine (free base)	2
13	Potassium iodide	0.83
14	Pyridoxine hydrochloride	0.5
15	Nicotinic acid (free acid)	0.5
16	Indole-3-acetic acid	0.5
17	Thiamine hydrochloride	0.4
18	Molybdic acid (sodium salt). $2H_2O$	0.25
19	Kinetin	0.04
20	Cobalt chloride. $6H_2O$	0.025
21	Cupric sulphate. $5H_2O$	0.025

The control sample was kept without treatment while the treated sample was handed over in sealed pack to Mr. Trivedi for the biofield energy treatment. Mr. Trivedi provided the biofield energy treatment to the treated group *via* his unique energy transmission process without touching the sample, under standard laboratory conditions. Subsequently, the treated and control samples were evaluated by various analytical techniques such as XRD, DSC, TGA-DTA, UV-vis, and FT-IR spectroscopy.

2.2. XRD Study

The XRD study of control and treated PMM samples was done on Phillips (Holland PW 1710) X-ray diffractometer. The system was equipped with copper anode and nickel filter while the wavelength was set to 1.54056Å. The percentage change in average crystallite size (G) was calculated with the help of following equation:

$$G = [(G_t - G_c)/G_c] \times 100 \qquad 1$$

Here, G_c and G_t are average crystallite size of control and treated powder samples, respectively.

2.3. DSC Study

The latent heat of fusion and melting temperature of control and treated PMM were determine with the help of Pyris-6 Perkin Elmer differential scanning calorimeter. The analyte samples were heated at the rate of 10ºC/min under air atmosphere with flow rate of 5 mL/min. An empty pan,

sealed with cover lid was used as a reference pan. The melting temperature (T_m) and latent heat of fusion (ΔH) were obtained from the DSC thermogram.

2.4. TGA-DTA Analysis

The TGA-DTA analysis of control and treated PMM samples was carried out on Mettler Toledo simultaneous TGA-DTA analyzer. The analytes were heated under air atmosphere from room temperature to 400ºC at the heating rate of 5ºC/min. The onset temperature of thermal degradation and temperature at which maximum weight loss occur (Tmax) in samples were obtained from the TGA-DTA thermogram.

2.5. UV-Vis Spectroscopic Analysis

The spectra of control and treated samples were acquired on Shimadzu UV spectrometer (2400 PC). The spectrometer was equipped with quartz cell of 1 cm, a slit width of 2.0 nm, and the wavelength was set to 200-400 nm.

2.6. FT-IR Spectroscopic Characterization

The FT-IR spectroscopy of control and treated samples of PMM was carried out to determine the effect of biofield energy treatment on molecular level like dipole moment, force constant, and bond strength in chemical structure [22]. The samples were prepared by crushing with spectroscopic grade KBr into fine powder and then pressed into pellets. The spectra were obtained from Shimadzu's Fourier transform infrared spectrometer (Japan) in the frequency region of 500-4000 cm-1.

3. Results and Discussion

3.1. XRD Analysis

The XRD diffractograms of PMM (control and treated) samples are shown in Fig. 1. The diffractograms showed the sharp and intense peaks of both control and treated samples that indicated the PPM was crystalline nature. The XRD diffractogram of control sample exhibited the peaks at Bragg's angle (2θ) equal to 18.89º, 23.42º, 23.68º, 29.25º, 32.18º, 32.51º, 33.65º, 33.88º, 40.99º, and 41.65º. Similarly, the XRD diffractogram of treated PMM exhibited the XRD peaks at 2θ equal to 18.95º, 23.50º, 23.75º, 29.34º, 32.31º, 32.62º, 33.58º, 33.77º, 41.08º, and 41.73º. The 2θ values showed the alteration in the 2θ angle of XRD peaks after biofield treatment as compared to the control. It is well reported that values of the 2θ angle might be altered due to presence of internal strain [23]. Based on this, it is presumed that biofield energy induced an internal strain in the treated sample that probably leads to alter its 2θ values with respect to the control sample. The average crystallite size was computed using following equation [24]:

$$\text{Scherrer Equation: } G = k\lambda/(b\cos\theta) \qquad 2$$

Here, λ is the wavelength of radiation used; b is full-width half maximum (FWHM); and k is the equipment constant (0.94). The average crystallite size of the control and treated samples were observed as 121.48 nm and 129.55 nm, respectively. The result showed about 6.64% increase in average crystallite size of the treated sample as compared to the control (Fig. 2). It is reported that increase in annealing temperature considerably affects the crystallite size of the compounds. This increase in temperature might lead to reduce the dislocation density and increase the number of unit cell, which ultimately increases the average crystallite size of sample [25, 26].

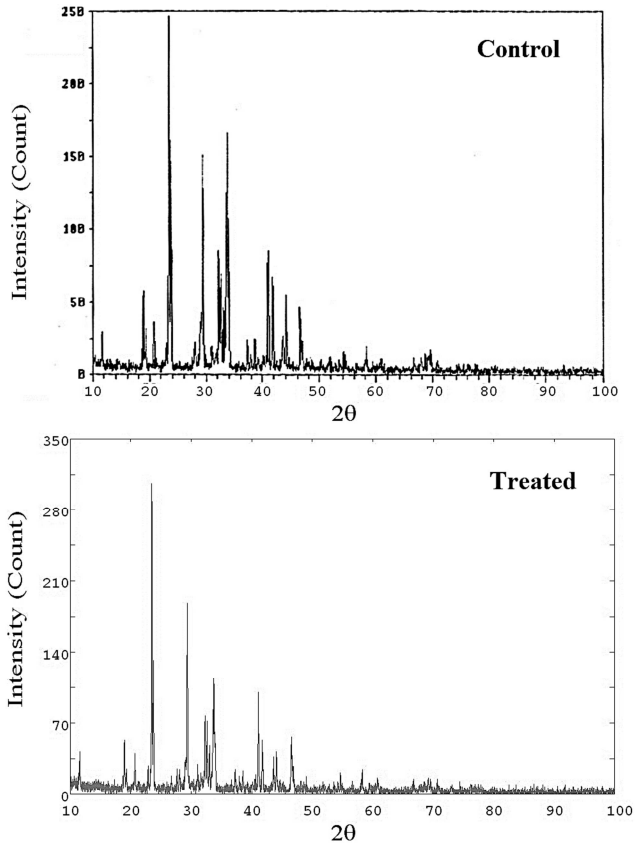

Fig. 1. *XRD diffractograms of potato micropropagation medium.*

Based on this, it is speculated that biofield treatment might supply some thermal energy to PMM molecules. This might lead to increase the average crystallite size of the treated sample as compared to the control sample.

3.2. DSC Analysis

DSC analysis was carried out to determine the latent heat of fusion (ΔH) and melting temperature of the treated and control samples of PMM. DSC thermograms of control and treated samples are shown in Fig. 3. The melting temperature of treated sample (131.38°C) was observed as very similar to that of control sample (131.85°C). However, the latent heat of fusion corresponding to control and treated samples was observed as 73.57 J/g and 67.20 J/g, respectively (Table 2). The result showed about 8.66% decrease in the latent heat of fusion of treated PMM with respect to the control. It is assumed that biofield energy might supply the energy, which

is stored in the treated sample.

This might lead to increase the ΔH of treated sample, as it required less energy for phase transition from solid to liquid with respect to the control. Previously, our group has been reported that biofield energy treatment has altered the value of ΔH in lead and tin powders [10].

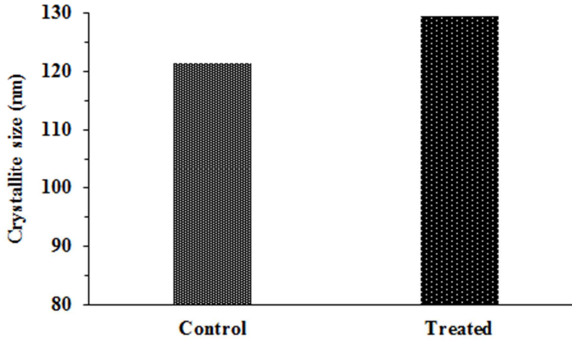

Fig. 2. *Average crystallite size of control and treated potato micropropagation medium.*

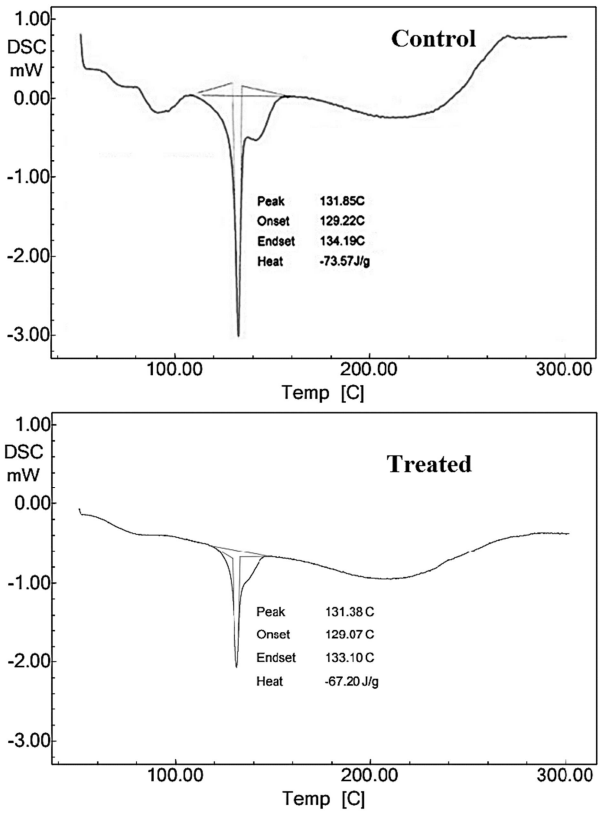

Fig. 3. *DSC thermograms of control and treated potato micropropagation medium.*

Table 2. *Thermal analysis of control and treated samples of potato micropropagation medium.*

Parameter	Control	Treated
Latent heat of fusion (J/g)	73.57	67.20
Melting point (ºC)	131.85	131.38
Onset temperature (ºC)	170.00	178.00
T_{max} (ºC)	207.50	218.00

T_{max}: temperature at maximum weight loss occurs

3.3. TGA-DTA Analysis

The TGA-DTA thermogram of control and treated PMM samples are shown in Fig. 4, and data is presented in Table 2.

The TGA thermogram of control sample showed the onset temperature of thermal degradation at 170°C, which was continued until 245°C (endset temperature). On the other hand, the TGA thermogram of the treated sample showed the onset temperature at 178°C and continued up to 251°C (endset temperature). The result showed about 4.71% increase in the onset temperature of thermal degradation of biofield energy treated sample as compared to the control. During the thermal degradation process, the maximum thermal degradation (T_{max}) was observed at 207.5°C (with 15.14% weight loss) in control and 218°C (with 6.47% weight loss) in the treated sample. This showed about 5.06% increase in T_{max} with respect to the control sample. Overall, this increase in onset temperature and T_{max} of treated sample might be due to the alteration in internal energy through biofield energy treatment, which results into enhanced thermal stability of treated sample as compared to the control [27].

3.4. FT-IR Spectroscopic Analysis

FT-IR spectra of the control and treated PMM are shown in Fig. 5. The PMM is composed with several mineral salts, vitamins, amino acids *etc*. Due to these different components, it contains several functional groups such as nitrate, sulfate, acids, aromatic ring etc. The FT-IR spectrum of control sample showed the vibrational peak at 3132 cm^{-1} that might be attributed to aromatic =C-H stretching. The peak was appeared as broad that might be due to overlap with the O-H stretching vibrations. In treated sample, the =C-H peak was observed at slight upstream region *i.e.* at 3161 cm^{-1}. The stretching frequency of any bond is directly proportional to the force constant and inversely proportional to reduced mass [28]. Therefore, it is presumed that biofield energy treatment might increase the dipole moment of =C-H bond as compared to the control sample. As a result, the force constant and bond strength of =C-H bonds might increase as compared to the control.

The FT-IR spectrum of control sample showed the IR peaks at 1760 cm^{-1} that was assigned to N=O bond [29]. This might be due to nitrate (potassium and ammonium) component of PMM. The peaks at 1398 and 825 cm^{-1} were attributed to asymmetric and symmetric vibration of NO_3 group, which is also due to the presence of potassium nitrate and ammonium nitrate as a source of nitrogen in PMM. In the FT-IR spectrum of treated sample, these vibrational peaks for N=O stretching, asymmetric NO_3 and symmetric NO_3 stretching appeared at 1760, 1400, and 825 cm^{-1}, respectively. The result showed the similar pattern of the vibrational frequency of nitrate group in both control and treated samples. The IR peaks at 1679 and 1141 cm^{-1} in control sample were attributed to C=O stretching and C-O stretching, respectively may be because of glycine present in PMM [30]. These peaks were appeared at the same frequency

region in treated sample. The vibrational peak at 1622 cm^{-1} in both control and treated sample might assigned to aromatic C=C stretching.

The IR peaks at 956-1004 cm^{-1} were assigned to S=O stretching, which might be due to presence of different sulfates salts such as zinc sulphate, cupric sulphate magnesium sulphate, manganese sulphate, ferrous sulphate *etc.* in PMM [31]. The peaks due to S=O bond in different sulfates are appeared at similar region *i.e.* 954-1001 cm^{-1} in the treated sample. The IR peaks at 603-663 cm^{-1} region were might be due to the Ca-Cl stretching in both control as well as treated samples of PMM [32]. Overall, the FT-IR study showed shifting of wavenumber of =C-H vibrations that might be due to increase of the force constant and bond strength of =C-H bonds in treated sample as compared to the control. The reset of vibrational peaks were observed at the similar region of IR frequency in both control and treated samples.

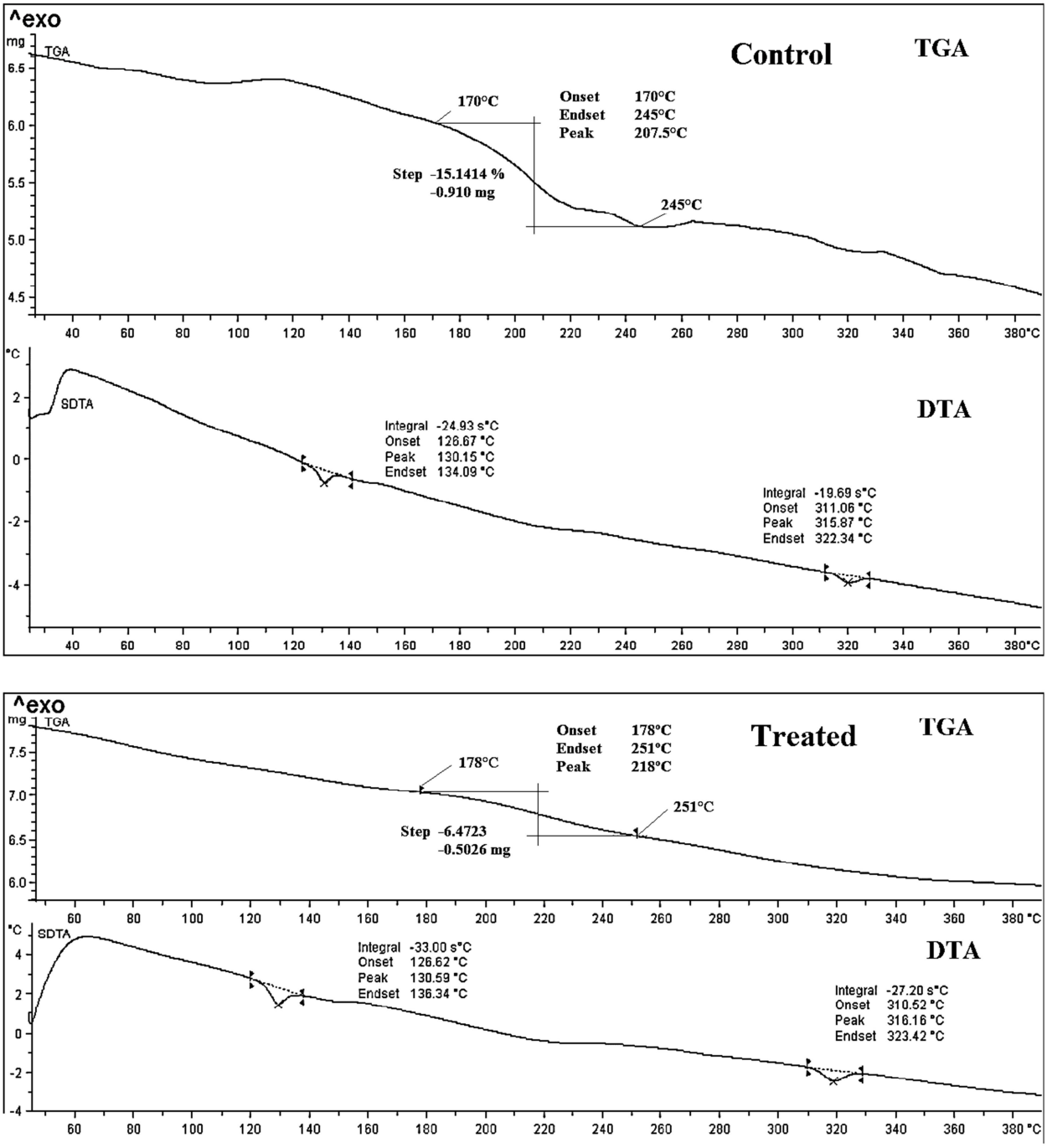

Fig. 4. *TGA-DTA thermograms of control and treated potato micropropagation medium.*

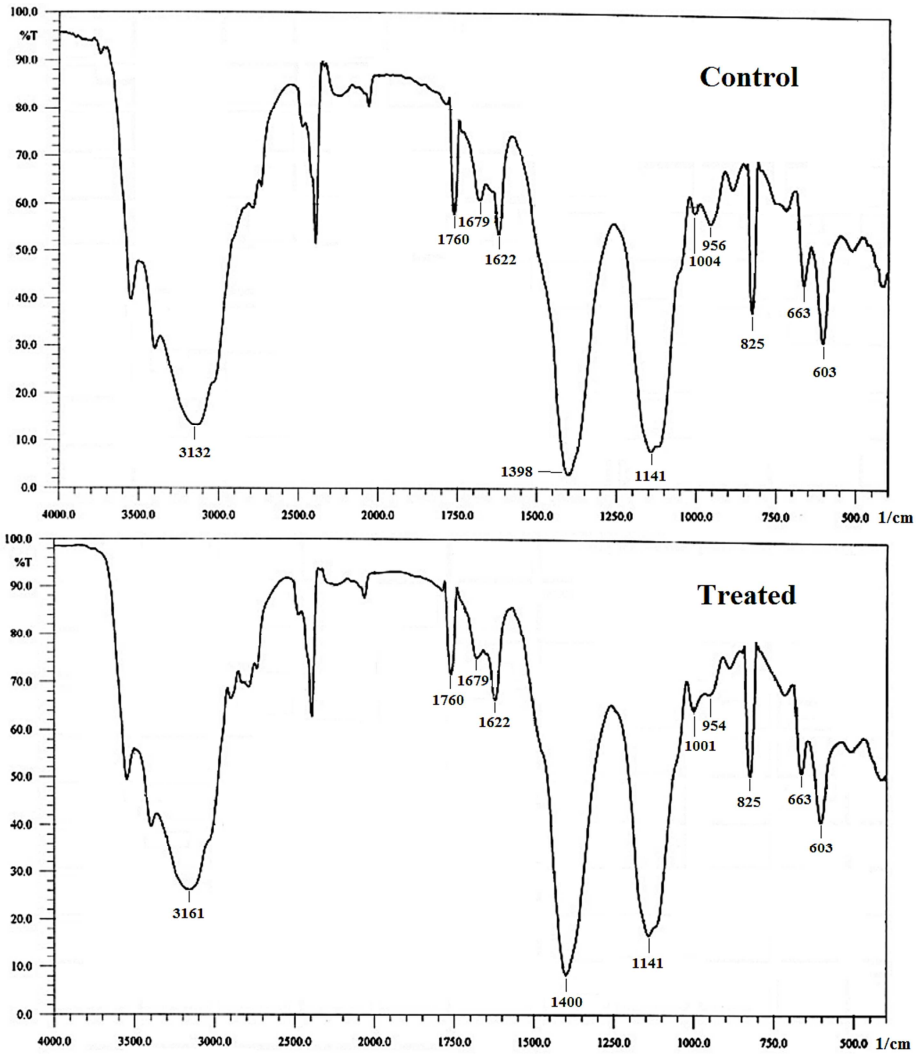

Fig. 5. *FT-IR spectra of control and treated potato micropropagation medium.*

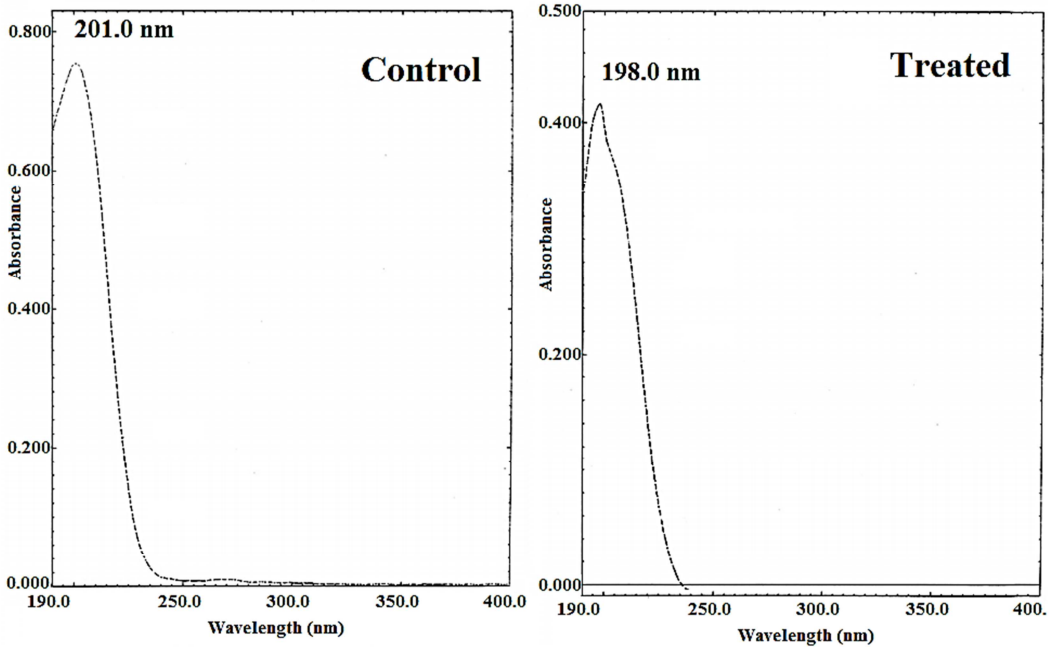

Fig. 6. *UV spectra of control and treated potato micropropagation medium.*

3.5. UV-Vis Spectroscopy

UV spectra of the control and treated PMM are shown in Fig. 6. The UV spectrum of control sample showed the absorbance maxima (λ_{max}) at 201.0 nm. Similarly, the UV spectra of treated sample showed the λ_{max} at 198.0 nm in treated sample. The result showed slight blue shift in the absorbance maxima in the treated sample as compared to the control.

The compound absorbs UV waves due to transition of electrons from stable state *i.e.* highest occupied molecular orbital (HOMO) to excited state *i.e.* lowest unoccupied molecular orbital (LUMO). When the HOMO-LUMO gap was altered, the λ_{max} was also altered correspondingly [22]. Based on this, it is presumed the HOMO-LUMO gap in treated sample has been increase, which required higher energy to overcome the electronic transition and thus the λ_{max} was shifted to higher energy (blue shift) as compared to the control.

4. Conclusion

In conclusion, the XRD study showed the crystalline nature of PMM in both the samples (control and treated). The intensity of XRD peaks and average crystallite size (6.64%) were increased after biofield energy treatment as compared to the control. The DSC study revealed the significant decrease in the latent heat of fusion (8.66%) in treated sample with respect to the control. The TGA-DTA study showed the slight increase in onset temperature as well as T_{max} by 4.71% and 5.06%, respectively with respect to the control. This showed the increase in thermal stability of treated PMM. The UV analysis revealed the slight blue shift in λ_{max} of treated sample with respect to the control. Moreover, the FT-IR analysis showed the increase in wavenumber of =C-H stretching after biofield treatment from 3132 cm^{-1} (control) to 3161 cm^{-1} (treated).

Overall, data suggest that Mr. Trivedi's biofield energy treatment showed the considerable impact on the physical, thermal and spectroscopic properties of PMM. Based on this, it is expected that Mr. Trivedi's biofield energy treatment can modulate the physicochemical properties of PMM so that it could be utilized as a better growth medium for the micropropagation of potato.

Abbreviations

NCCAM: National Center for Complementary and Alternative Medicine;
NIH: National Institute of Health;
XRD: X-ray diffraction;
TGA: Thermogravimetric Analysis;
DTA: Differential thermal analysis

Acknowledgement

The authors would like to thank the Trivedi Science, Trivedi Master Wellness and Trivedi Testimonials for their support during the study. Authors would also like to acknowledge the entire scientific team of MGV pharmacy college, Nashik for allowing the instrumental facility.

References

[1] Singh HP, Uma S, Selvarajan R, Karihaloo JL (2011) Micropropagation for production of quality banana planting material in Asia-Pacific. Asia-Pacific Consortium on Agricultural Biotechnology (APCoAB), New Delhi.

[2] Thomas P, Reddy KM (2013) Microscopic elucidation of abundant endophytic bacteria colonizing the cell wall–plasma membrane peri-space in the shoot-tip tissue of banana. AoB PLANTS 5: plt011.

[3] Tikole SS, Kakade TB, Shelar DB, Bamane GS, Bite MV, et al. (2014) Transgenic plants: The new promising approach. World J Pharm Pharm Sci 3: 316-332.

[4] Ahmed Z, Akhter F, Haque MS, Banu H, Rahman MM, et al. (2001) Novel micropropagation system. J Biol Sci 11: 1106-1111.

[5] Rabbani A, Askari B, Abbasi NA, Bhatti M, Quraishi A (2001) Effect of growth regulators on *in vitro* multiplication of potato. Int J Agric Biol 3: 181-182.

[6] Abdelaleem KG (2015) *In vitro* organogenesis of (*Solanum tuberosum* L.) plant cultivar alpha through tuber segment explants callus. Int J Curr Microbiol App Sci 4: 267-276.

[7] Tovar P, Dodds JH (1986) Tissue culture propagation of potato. CIP slide training series 1-5 int. Potato center, Dept. of training and communications, Lima, Peru.

[8] http://www.himedialabs.com/TD/PT090.pdf.

[9] Lenssen AW (2013) Biofield and fungicide seed treatment influences on soybean productivity, seed quality and weed community. Agricultural Journal 8: 138-143.

[10] Trivedi MK, Patil S, Tallapragada RM (2013) Effect of bio field treatment on the physical and thermal characteristics of silicon, tin and lead powders. J Material Sci Eng 2: 125.

[11] Koithan M (2009) Introducing complementary and alternative therapies. J Nurse Pract 5: 18-20.

[12] Rubik B (2008) Measurement of the Human biofield and other energetic instruments, Chapter 20 of energetics and spirituality by Lyn Freeman. http://www.faim.org/energymedicine/measurement-human-biofield.html.

[13] Ho MW (1995) Bioenergetics and the coherence of organisms. Neuronetwork World 5: 733-750.

[14] Gough WC (1999) The cellular communication process and alternative modes of healing. Subtle Energies Energy Med 8: 67-101.

[15] Warber SL, Cornelio D, Straughn J, Kile G (2004) Biofield energy healing from the inside. J Altern Complement Med 10: 1107-1113.

[16] Chang PL (2015) What is the human biofield and the role of biophotons? http://energyfanatics.com/2015/01/02/what-is-human-biofield-role-biophotons.

[17] Stenger VJ (1999) Bioenergetic fields. Sci Rev Alternative Med 3. http://www.colorado.edu/philosophy/vstenger/Medicine/Biofield.html

[18] Shinde V, Sances F, Patil S, Spence A (2012) Impact of biofield treatment on growth and yield of lettuce and tomato. Aust J Basic Appl Sci 6: 100-105.

[19] Sances F, Flora E, Patil S, Spence A, Shinde V (2013) Impact of biofield treatment on ginseng and organic blueberry yield. Agrivita, J Agric Sci 35.

[20] Nayak G, Altekar N (2015) Effect of biofield treatment on plant growth and adaptation. J Environ Health Sci 1: 1-9.

[21] Trivedi MK, Nayak G, Patil S, Tallapragada RM, Jana S, et al. (2015) Bio-field treatment: An effective strategy to improve the quality of beef extract and meat infusion powder. J Nutr Food Sci 5: 389.

[22] Pavia DL, Lampman GM, Kriz GS (2001) Introduction to spectroscopy. (3rdedn), Thomson Learning, Singapore.

[23] Fultz B, Howe JM (2002) In Transmission electron microscopy and diffractometry of materials. Diffraction and the X-ray powder diffractometer. (4thedn), Springer-Verlag: Berlin.

[24] Alexander L, Klug HP (1950) Determination of crystallite size with the X-ray spectrometer. J App Phys 21: 137-142.

[25] Gaber A, Abdel-Rahim MA, Abdel-Latief AY, Abdel-Salam MN (2014) Influence of calcination temperature on the structure and porosity of nanocrystalline SnO_2 synthesized by a conventional precipitation method. Int J Electrochem Sci 9: 81-95.

[26] Raj KJA, Viswanathan B (2009) Effect of surface area, pore volume, particle size of P25 titania on the phase transformation of anatase to rutile. Indian J Chem Sec A 48A: 1378-1382.

[27] Spear RJ, Maksacheff M (1986) The relationship between ignition temperature and thermal stability for selected primary explosives. Thermochim Acta 105: 287-293.

[28] Smith BC (1998) Infrared spectral interpretation: A systematic approach. CRC Press.

[29] Miller FA, Wilkins CH (1952) Infrared spectra and characteristic frequencies of inorganic ions. Anal Chem 24: 1253-1294.

[30] Blout ER, Linsley SG (1952) Infrared spectra and the structure of glycine and leucine peptides. J Am Chem Soc 74: 1946-1951.

[31] Chaban GM, Huo WM, Lee TJ (2002) Theoretical study of infrared and Raman spectra of hydrated magnesium sulfate salts. The J Chem Phys 117: 2532-2537.

[32] Nirmala R, Nam KT, Navamathavan R, Park SJ, Kim HY (2011) Hydroxyapatite mineralization on the calcium chloride blended polyurethane nanofiber *via* biomimetic method. Nanoscale Res Lett 6: 2.